Biochemistry

Article

Cite This: Biochemistry 2018, 57, 3244−3251

pubs.acs.org/biochemistry

Lactate Racemase Nickel-Pincer Cofactor Operates by a Proton-Coupled Hydride Transfer Mechanism

Joel A. Rankin,[†] Robert C. Mauban,[⊥] Matthias Fellner,[†] Benoît Desguin,[‡] John McCracken,*[,§] Jian Hu,*[,†,§] Sergey A. Varganov,*[,⊥] and Robert P. Hausinger*[,†,∥]

[†]Department of Biochemistry and Molecular Biology, [§]Department of Chemistry, and [∥]Department of Microbiology and Molecular Genetics, Michigan State University, East Lansing, Michigan 48824, United States

[⊥]Department of Chemistry, University of Nevada, Reno, Nevada 89557, United States

[‡]Institute of Life Sciences, Université catholique de Louvain, B-1348 Louvain-La-Neuve, Belgium

Supporting Information

ABSTRACT: Lactate racemase (LarA) of *Lactobacillus plantarum* contains a novel organometallic cofactor with nickel coordinated to a covalently tethered pincer ligand, pyridinium-3-thioamide-5-thiocarboxylic acid mononucleotide, but its function in the enzyme mechanism has not been elucidated. This study presents direct evidence that the nickel-pincer cofactor facilitates a proton-coupled hydride transfer (PCHT) mechanism during LarA-catalyzed lactate racemization. No signal was detected by electron paramagnetic resonance spectroscopy for LarA in the absence or presence of substrate, consistent with a +2 metal oxidation state and inconsistent with a previously proposed proton-coupled electron transfer mechanism. Pyruvate, the predicted intermediate for a PCHT mechanism, was observed in quenched solutions of LarA. A normal substrate kinetic isotope effect (k_H/k_D of 3.11 ± 0.17) was established using 2-α-^{2}H-lactate, further supporting a PCHT mechanism. UV−visible spectroscopy revealed a lactate-induced perturbation of the cofactor spectrum, notably increasing the absorbance at 340 nm, and demonstrated an interaction of the cofactor with the inhibitor sulfite. A crystal structure of LarA provided greater resolution (2.4 Å) than previously reported and revealed sulfite binding to the pyridinium C4 atom of the reduced pincer cofactor, mimicking hydride reduction during a PCHT catalytic cycle. Finally, computational modeling supports hydride transfer to the cofactor at the C4 position or to the nickel atom, but with formation of a nickel-hydride species requiring dissociation of the His200 metal ligand. In aggregate, these studies provide compelling evidence that the nickel-pincer cofactor acts by a PCHT mechanism.

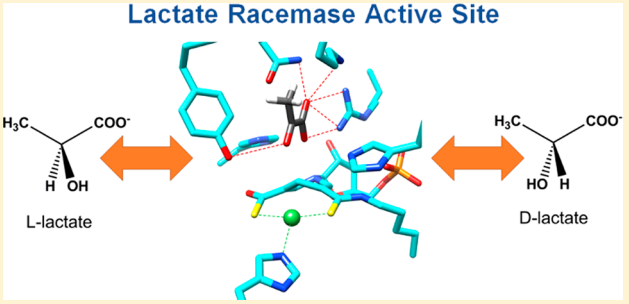

Lactate racemase (LarA), a microbial enzyme that interconverts the D- and L-isomers of lactic acid (Scheme 1), was first reported for intact cells of two *Clostridium* species

Scheme 1. Reaction Catalyzed by Lactate Racemase

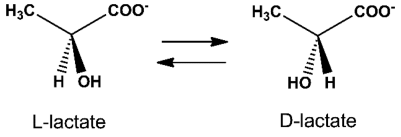

in 1936,[1] but only recently was it shown to possess a covalently tethered, nickel-containing cofactor derived from nicotinic acid adenine dinucleotide and synthesized by LarB, LarC, and LarE.[2−7] Structural characterization of LarA from *Lactobacillus plantarum* revealed a pyridinium-3-thioamide-5-thiocarboxylic acid mononucleotide attached to Lys184 of the protein, with the two sulfur atoms and the pyridinium C4 carbon atom bound to nickel as an (SCS) pincer complex with additional metal coordination by His200 (Scheme 2). Two nearby histidine residues, His108 and His174, are well positioned to

Scheme 2. Nickel-Pincer Cofactor of LarA

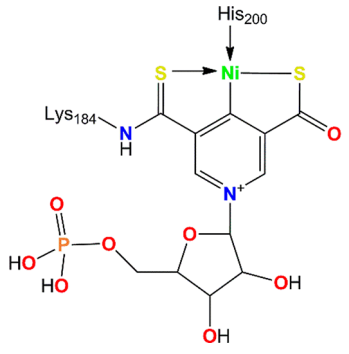

Special Issue: Current Topics in Mechanistic Enzymology

Received: January 29, 2018
Revised: February 28, 2018
Published: February 28, 2018

DOI: 10.1021/acs.biochem.8b00100
Biochemistry 2018, 57, 3244−3251

Scheme 3. Potential Proton-Coupled Hydride Transfer (PCHT) Mechanism of LarA

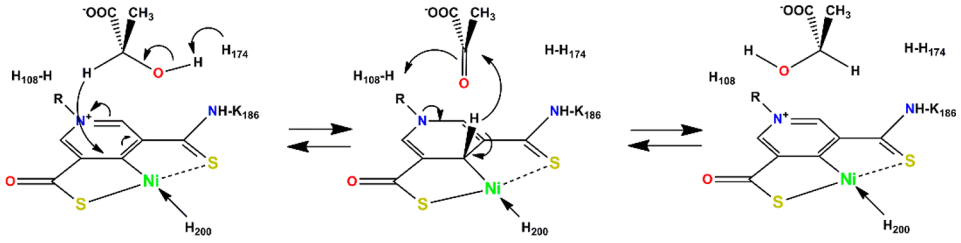

participate in catalysis by acting as general acids/bases, and their substitutions by alanine residues leads to enzyme inactivation.[2] The LarA structure is consistent with a proton-coupled hydride transfer (PCHT) mechanism (Scheme 3), in which one of the nearby histidine residues abstracts the hydroxyl group proton of lactate, a hydride transfers to the nickel-pincer cofactor with formation of bound pyruvate, and the hydride returns to either face of the ketoacid with proton donation by the opposite histidine residue resulting in racemization. This scheme depicts hydride transfer to C4 of the pyridinium ring, similar to what is observed in NAD/NMN-dependent enzymes;[8] however, hydride transfer to the metal was also considered in the original report.[2] Indeed, the ability for hydride to localize either to the C4 position or to the nickel ion could potentially help explain the loss of stereospecificity for hydride return to pyruvate.[9] Direct experimental evidence for a PCHT mechanism has not been reported.

The elucidation of the LarA crystal structure inspired the synthesis of an (SCS) nickel-pincer model compound that closely resembles the enzyme metallocenter.[10] The nickel-containing 1-methyl-3,5-dithioamide-pyridinium species reacts with several primary and secondary alcohols to catalyze dehydrogenation reactions, forming the corresponding aldehydes and ketones. The authors carried out density functional theory (DFT) calculations indicating the reactions likely take place via hydride transfer to C4 of the pyridinium ring, and product analyses demonstrated the subsequent loss of nickel with rearomaticization of the ring.

Four other computational studies have addressed the mechanism by which the nickel-pincer cofactor facilitates the racemization of lactic acid. Zhang and Chung used DFT with M06, B3LYP-D3, and TPSSh-D3 methods to examine 63- and 139-atom models of the active site.[11] Their results are consistent with direct hydride transfer to the pyridinium C4 atom (Scheme 3), whereas their calculations are kinetically and thermodynamically inconsistent with hydride transfer to the nickel atom or to C8, and the authors report that His174 partially blocks hydride transfer to C7. Replacement of the nickel atom with cobalt leads to higher energy barriers, while replacing the nickel with a proton or eliminating the tether lowers the energy barriers and increases the thermodynamic stability of the pyruvate intermediate. The authors proposed that destabilization of the intermediate is important to the racemization reaction. In addition, they suggested the involvement of His174 and His108 as alternate bases reacting with the different lactate isomers, as earlier proposed from the crystal structure.[2] Yu and Chen used the B3LYP-D3 method to study a 200-atom model of the active site.[12] Their calculations show no indication of a two-step mechanism (i.e., it is a coupled reaction) and support a mechanism involving PCHT to C4 of the pyridinium ring (Scheme 3), while failing to transfer hydride to the nickel atom. In addition, these investigators found that the nickel pincer exhibited stronger hydride-addition reactivity compared to NAD^+ in environments of medium to high polarity. Qiu and Yang compared the predicted reactivities of several scorpion-like nickel-pincer complexes (independent of a protein environment) possessing tails that provide a reactive imidazole group.[13] Their calculations position the hydride on the pyridinium C4 atom and show increasing energy barriers as one shifts from a symmetric dithioamide pyridinium−Ni-Cl to asymmetric thioamide/thioacid pyridinium-Ni-CO to a dithioamide pyridinium−Pd-Cl to a dithiophosphine pyridinium−Pd-Br to a dithioamide benzyl−Ni-Cl species; thus, nickel is better than palladium and replacement of the pyridinium ring nitrogen by carbon is deleterious. In contrast to these three publications focused on PCHT, Wang and Shaik proposed an intriguing proton-coupled electron transfer (PCET) mechanism for the LarA reaction (Scheme 4).[14] These investigators used quantum

Scheme 4. Postulated Proton-Coupled Electron Transfer Mechanism of LarA

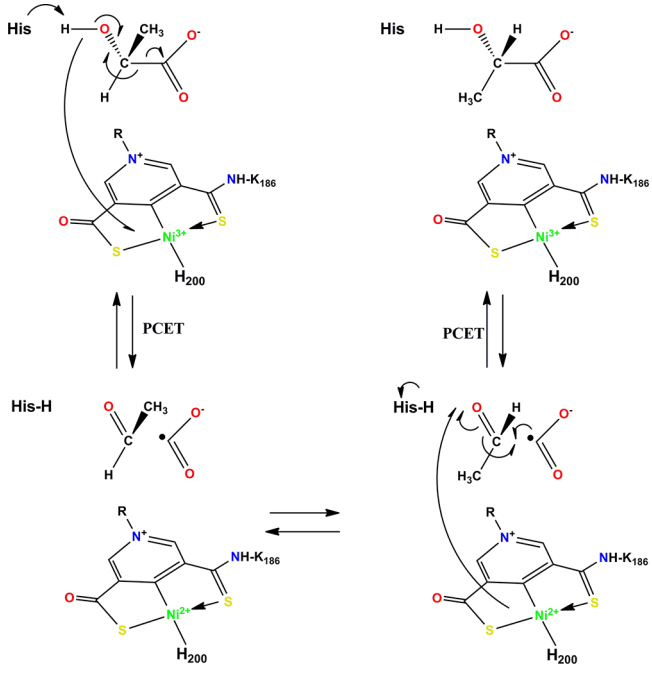

mechanics/molecular mechanics (QM/MM) calculations in which the QM component used a hybrid UB3LYP functional while performing MM on the entire protein. They suggested the metal initially possesses a Ni(III) redox state that is reduced to Ni(II) during the reaction, with the C1−C2 bond of lactate being transiently cleaved to yield a CO_2 radical anion and acetaldehyde that rotates, followed by reversal of the preceding

DOI: 10.1021/acs.biochem.8b00100
Biochemistry 2018, 57, 3244−3251

steps. Taken together, it is clear that computational efforts have not established the mechanism.

Here, we provide experimental evidence in direct support of a PCHT mechanism of lactate racemase, we present a new crystal structure of LarA at better resolution that also supports a PCHT mechanism, and we provide computational support that the hydride can transfer to the nickel as well as the pyridinium C4 atom.

EXPERIMENTAL PROCEDURES

LarA Purification, Activity, and Nickel Content. C-Terminal Strep II-tagged LarA of *L. plantarum* was isolated from *Lactococcus lactis* strain NZ3900 containing plasmid pGIR112 with the modified *larA* and *larBCDE* under control of the *nisA* promoter.[4] Overnight starter cultures were grown at 30 °C in M17 medium supplemented with 0.5% w/v D-glucose and 10 mg/L chloramphenicol, then were used to inoculate (at 1% final volume) larger volumes of the same medium with 5 mg/mL of chloramphenicol at 28 °C with mild shaking. At an OD_{600} of 0.2−0.3, cultures were induced with 10 μg/L nisin A, supplemented with 1 mM $NiCl_2$, and grown for 4 h before collection by centrifugation and storage at −80 °C.

Cell pellets (5−10 g) were thawed and diluted to 40 mL of 100 mM Tris-HCl, pH 7.5, containing 150 mM NaCl, 0.5 mM Na_2SO_3 (which stabilizes the enzyme activity),[2] 1 mM phenylmethylsulfonyl fluoride (using 100 mM stock dissolved in ethanol), and 2.5 U/mL benzonase, with, in some cases, 5 mM ascorbic acid. The cells were disrupted by two passes through a French pressure cell (16 000 psi) that had been prechilled to 4 °C. Cell-free lysates were obtained after centrifugation at 27000*g* for 40 min at 4 °C. The lysates were applied at 4 °C to 2 mL of StrepTactin superflow or StrepTactin XT resin (IBA) equilibrated in 100 mM Tris-HCl, pH 7.5, containing 150 mM NaCl, 0.05 mM Na_2SO_3, and, in some cases, 5 mM ascorbic acid. After the resins were washed with three column volumes of buffer, the enzyme was eluted with buffer containing either 5 mM desthiobiotin or 50 mM biotin, respectively. Alternatively, the LarA used in the crystallization experiments was purified as previously described.[2]

LarA activity was assayed by measuring the conversion of D- to L-lactate or L- to D-lactate using isomer specific dehydrogenases in a commercial kit (Megazyme) as previously described.[4] Protein concentrations were assessed by the Bradford assay.[15]

Electron Paramagnetic Resonance (EPR) Spectroscopy. Sulfite, a LarA inhibitor, was diluted to less than 100 nM in the protein sample by using an Ultra-4 10 kDa cutoff centrifugal filter (Amicon) to carry out two dilution/concentration buffer exchanges into 100 mM Tris-HCl, pH 7.5, containing 150 mM NaCl and 5 mM ascorbic acid. The sample was adjusted to 25% glycerol (w/v) in a volume of 160 μL containing 3.6 mg/mL (75 μM) of LarA and frozen in liquid N_2. After initial spectroscopic analysis, the sample was thawed, 16 μL of 1 M D-lactate was added and mixed, and the modified sample was refrozen.

Continuous-wave EPR measurements were made at X-band on a Bruker E-680X spectrometer using a Bruker SHQ probe fitted with an Oxford ESR 900 liquid helium cryostat. Measurement conditions were microwave frequency, 9.407 GHz; sample temperature, 8 K; magnetic field scan range, 150−450 mT; magnetic field modulation amplitude, 1.0 mT, modulation frequency, 100 kHz. Microwave powers were varied from 0.1−1.0 mW and video gains ranged from 70−90 dB.

UV−Visible Spectroscopy. UV−visible absorbance spectra were obtained using a Shimadzu UV-2600 spectrophotometer. Purified LarA was separated from sulfite by using a PD-10 column (GE Healthcare) to exchange into 20 mM Tris-HCl, pH 7.5, containing 150 mM NaCl and the spectrum was collected for a 200-μL sample (0.94 mg/mL) using a microcuvette. To this sample was added either 20 μL of 1 M sodium D-lactate and then 20 μL of 100 mM Na_2SO_3 or just the sulfite with spectra collected after each addition corrected for dilution.

Pyruvate Detection. To eliminate contaminating pyruvate, stock solutions of lactate (either the L-isomer or D-isomer) were brought to high pH with NaOH, treated overnight with excess $NaBH_4$, and acidified with HCl.

LarA was buffer exchanged at 4 °C into deoxygenated, argon-equilibrated 20 mM Tris-HCl, pH 7.5, containing 150 mM NaCl by twice using a PD-10 column (GE Healthcare) followed by concentration using an Ultra-4 10-kDa centrifugal filter. The LarA samples (1−6 mg/mL) were mixed on ice with pyruvate-free lactate (200 mM final concentration) in 60 mM MES-NaOH, pH 6.0, and incubated at 30 °C for 2 min. The reactions were quenched by adding an equal volume of ice-cold 0.5 M perchloric acid, and the mixtures were kept on ice for 5 min, neutralized with 250 mM K_2CO_3, and incubated on ice. The protein was removed by centrifugation (17000*g*, 1 min), and the supernatants were used in pyruvate assays as previously described.[16] Briefly, 20 μL of the supernatant was diluted to 200 μL in 100 mM potassium phosphate, pH 6.7, containing 1 mM Na-EDTA, 1 mM $MgCl_2$, 0.2 U/mL of pyruvate oxidase (MP Biomedical), 0.2 U/mL of horseradish peroxidase (HRP, Sigma Chemical Co.), and 50 μM 10-acetyl-3,7-dihydroxyphenoxazine (Cayman Chemical) in an opaque black microtiter plate. The assay was incubated at room temperature for 30 min, and the fluorescence was examined with a PerkinElmer EnVision 2104 plate reader using 530 nm excitation and 590 nm emission. The fluorescence intensities obtained for sample pyruvate concentrations were compared to those of a pyruvate standard curve.

As an independent approach to investigate the LarA intermediate, the protein samples used for the fluorescence assay were treated with perchloric acid (250 mM) as described earlier to precipitate the protein, and the remaining solution was derivatized with 2,4-dinitrophenylhydrazine (DNPH) by a method adapted from a previously described protocol.[17] In brief, 20 μL of the acidified solution was mixed with 10 μL formic acid, 100 μL of DNPH dissolved in water (0.1 mg/mL), and 180 μL of acetonitrile. The reaction mixture was incubated at 37 °C for 1 h, and then twice extracted with 600 μL of a 1:5 solution of ethyl acetate:hexanes. The combined uppermost layer was dried using a SpeedVac at 42 °C and dissolved in 100 μL of methanol. Liquid chromatographic separation of the sample (10 μL injection volume) was performed with a Waters Aquity UPLC system using a C18 column (Aquity BEH 1.7 μm, 2.1 × 100 mm) and mobile phases 0.15% formic acid in water (A) and acetonitrile (B). The gradient elution (0.3 mL/min) used the following program: 0−7 min, 1% B to 99% B; 7−9 min isocratic at 99% B; and 9−10 min, 1% B. Electrospray ionization-quantitative time-of-flight mass spectrometry used a XEVO G2-XS in negative ionization mode.

Substrate Kinetic Isotope Effect. The substrate kinetic isotope effect for 2-^{2}H-L-lactate was examined by incubating

DOI: 10.1021/acs.biochem.8b00100
Biochemistry 2018, 57, 3244−3251

purified and sulfite-free LarA with 20 mM solutions of the sodium form of deuterated sample (CDN Isotopes) or non-deuterated L-lactate (Sigma) in 60 mM MES-NaOH, pH 6.0, for 10 min at 35 °C. The reactions were terminated by incubating at 95 °C for 10 min. The concentrations of D-lactate in the samples were determined as described earlier.

Structural Characterization of LarA. LarA was crystallized in 0.1 M Bis-Tris buffer (pH 6.5) containing 2 M ammonium sulfate. X-ray diffraction data were collected at the Advanced Photon Source GM/CA beamline 23-ID-D. Data sets were processed, merged, and scaled with HKL2000.[18] The phases were solved by Phaser molecular replacement in Phenix[19] using PDB entry 5HUQ[2] as the template. Model building and refinement were conducted in COOT[20] and Phenix.[19]

We started out modeling all chains with sulfates and the nonreduced cofactor as in our earlier structure.[2] Although this approach worked well in chain B, it did not fit the density in chains A and C and also led to clashing with the pyridinium C4 atom in both cases. Examining the mF_o-DF_c map without a modeled ligand showed that the outward-facing density above the ring was more flat in chains A and C, while that in chain B appeared more round and the center of the density in chain B also was further away from the cofactor when comparing chain A to chain B. Lastly, the density of the ring and the molecule above it was apparently connected in chain A, but less so in chain B and again with chain C being in the middle. An attempt to model sulfite and the nonreduced cofactor in chains A and C fit the density nicely; however, refining the sulfite correctly with the observed density remained challenging, especially in chain A. We therefore produced the model of the reduced cofactor and a covalent bond in A, which was refined very well and matched the density best. The reduced sulfite-modified version of the cofactor (pyridinium-3,5-bisthiocarboxylic acid mononucleotide or P2TMN) was created with Jligand.[21] The model and structure factors were deposited in the PDB under ID 6C1W. Statistics for the data set are listed in Table S1. Structure analysis and figures were created with UCSF Chimera.[22]

Computational Methods. Two types of active site models were considered. Large models were used to calculate the reaction barriers for PCHT to the pyridinium C4 atom. The goal was to obtain the reaction barriers for different models using the same model size and level of theory. To this end, the model of Zhang and Chung[11] and the model of Yu and Chen[12] were reduced to 98 and 97 atoms, respectively. The 98-atom model contained the protonated Lys298 residue, while in the 97-atom model this residue was neutral, as in the original studies. To obtain these models, where necessary the single C−C bonds were cut and capped with hydrogen atoms. Only the positions of these hydrogen atoms were reoptimized, while positions of all other atoms were kept frozen. To predict the reaction barriers, the same procedure was applied to the reactant and transition state structures (Tables S2−S6). Two small models with 34 atoms (with His200) and 22 atoms (without His200) were used to investigate the possibility of hydride binding to nickel (Tables S7−S14). For all models except the small model with neutral His200, the total charge and electron spin were set to 0. The charge and spin of the model with neutral His200 were set to +1 and 0, respectively. Electronic structure calculations on the large models were carried out with the unrestricted B3LYP-D3 method and def2-SVP basis set. Calculations on the small models were performed without D3 dispersion correction and with the slightly smaller def2-SV(P) basis set. In all calculations, the protein environment was simulated with the polarization continuum model using the dielectric constant $\varepsilon = 4$, the solvent radius $r_{solv} = 1.20$ Å, and the nickel radius $r_{Ni} = 1.63$ Å. All calculations were performed with the GAMESS suite of programs.[23]

RESULTS AND DISCUSSION

EPR Analysis of LarA. A key distinction between the postulated PCHT and PCET mechanisms for LarA is the redox state of nickel in the enzyme. Whereas the mechanisms that invoke hydride transfer to the nickel-pincer cofactor assume the more stable Ni(II) state, the PCET mechanism invokes the more oxidized Ni(III) state for the starting enzyme, with intermediate states containing Ni(II). To test the redox state of the metal in LarA, we examined the sample lacking and containing substrate by EPR spectroscopy. A square planar nickel in the +2 oxidation state, as indicated by the crystal structure, would yield a diamagnetic species. By contrast, Ni(III) sites are typically octahedral or tetragonal and give rise to signals in the region from $g = 2.4-2.0$. Our measurements show no EPR signal over the 150−450 mT region scanned, consistent with diamagnetic Ni(II) in the samples.

UV−Visible Spectroscopic Analyses of LarA. The spectrum of sulfite-free LarA exhibited electronic transitions at 380 and 440 nm with a shoulder at 550 nm (Figure 1A). The addition of lactate led to absorbance increases at 340 and 400 nm along with a broad feature at 600 nm, as most easily visualized by the difference spectrum. The 340 nm transition associated with lactate addition to LarA (Figure 1A) matches

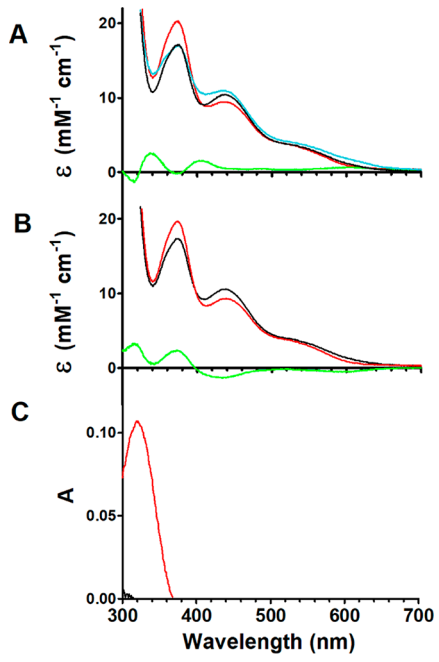

Figure 1. Lactate and sulfite alter the UV−visible spectrum of LarA. (A) Spectrum of LarA (black trace) and spectra obtained by sequential addition of lactate (cyan trace) then sulfite (red trace). Also shown is the difference spectrum for the changes when lactate is added (green trace). (B) Spectrum of LarA (black trace) and that obtained after adding sulfite (red trace), along with the difference spectrum (green trace). (C) Spectrum of NAD^+ before (black trace) and after addition of sulfite (red trace).

DOI: 10.1021/acs.biochem.8b00100
Biochemistry 2018, 57, 3244−3251

the wavelength of the spectrum obtained by hydride addition to C4 of NAD^+ (with ~10% of the NADH extinction coefficient as expected for a partially reduced state), consistent with hydride addition to C4 of the nickel-pincer cofactor. The addition of sulfite to LarA containing lactate (Figure 1A) or directly added to LarA (Figure 1B) resulted in an intensification of the 380 nm electronic transition and a diminishment of the absorbance at 440 nm. The resulting 440 nm/380 nm absorbance ratio matches that of the previously reported chromophore for the enzyme that was in buffer containing 50 μM sulfite.[2] The 320 nm transition formed by sulfite addition to LarA (Figure 1B) is consistent with that formed by sulfite interaction with NAD^+ (Figure 1C), suggesting attack at C4 of the nickel-pincer cofactor. We cannot yet assign the longer wavelength transitions of the Ni-pincer cofactor.

Characterization of the LarA Intermediate. A critical distinction between the PCHT and PCET mechanisms is the identity of the organic intermediate, pyruvate versus acetaldehyde, respectively. Pyruvate was present in enzyme samples that were mixed with borohydride-treated lactate substrate, quenched, and assayed by using a pyruvate oxidase/HRP coupled system. The amount of pyruvate detected varied with the enzyme preparation and corresponded to a mole fraction of 5−30% compared to the amount of LarA. To take account of the enzyme specific activity for each preparation, thus circumventing the batch-to-batch variation, a consistent amount of pyruvate per unit of enzyme activity was observed (Figure 2). This result indicates that a significant fraction of

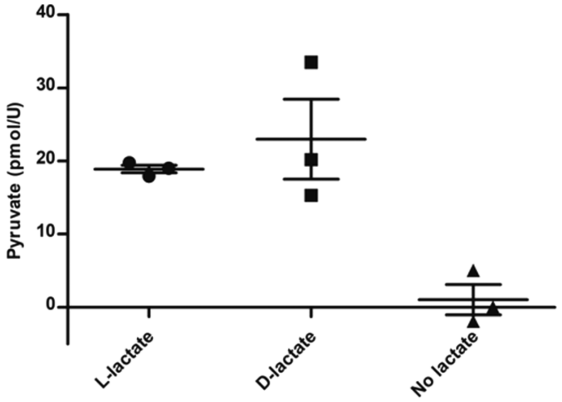

Figure 2. Detection of pyruvate as an intermediate in the LarA reaction. The amount of pyruvate was determined after quenching the reaction using 40−130 μM enzyme and 200 mM D- or L-lactate and a lactate-free control. The amount of pyruvate was quantified on the basis of the measured enzyme activity units (D- to L-conversion).

LarA is in the reduced, pyruvate-bound state under near saturating conditions of substrate. Such a result argues against a destabilized intermediate state, as suggested by one computational study.[11]

A mass spectrometry method involving DNPH derivatization of quenched LarA samples confirmed that pyruvate formed from D-lactate during the reaction (Figure S1). These findings are consistent with the intermediacy of pyruvate and consistent with a hydride transfer mechanism.

Substrate Kinetic Isotope Effect (KIE) Studies. Long before the elucidation of the LarA crystal structure, experimentalists had studied the mechanism of lactate racemase by examining substrate kinetic isotope effects using the enzyme from *Clostridium beijerinckii*. Specifically, Shapiro and Dennis examined the D- and L-isomers of 2-α-^{2}H-lactic acid to reveal k_H/k_D values of 2.16 and 2.14, respectively.[24] These KIEs are consistent with direct cleavage of the C−H bond in the substrate as expected for the hydride transfer mechanism (Scheme 3), but they are inconsistent with the PCET mechanism where this bond remains intact (Scheme 4). These researchers also showed the product retained ^{2}H, consistent with either mechanism. Although *C. beijerinckii* possesses two genes encoding LarA-like proteins,[4] neither of these proteins have been connected to the cell's lactate racemase activity.

To directly examine the substrate KIE for LarA from *L. plantarum*, we compared the reaction rates using nonlabeled and 2-α-^{2}H-lactic acid. The measured k_H/k_D of 3.11 ± 0.17 is consistent with a normal KIE (e.g., values of 3−5 typically are associated with hydride transfer in NAD^+ enzymes)[25] and supports the PCHT mechanism in which the C−H is broken and reformed during catalysis.

Structural Characterization of LarA in Complex with Sulfite. The published structure for LarA (5HUQ) solved at a moderate resolution (3 Å) revealed two chains per asymmetric unit with a closed conformation containing a buried nickel-pincer cofactor and a more open conformation with a metal-free pincer cofactor that was accessible to solvent.[2] A new crystal form of the same construct provided a structure with improved resolution (2.40 Å) where the three chains in one asymmetric unit occur in the closed conformation, with RMSD of ~0.3−0.4 Å between the three chains and the closed chain of the previous model (5HUQ). The only overall backbone difference occurs at the C-terminal *Strep* II-tag.

As with the previously described closed conformation, all three chains in the current structure contain the nickel-pincer complex. Nearly all protein side chains at the active site pocket (residues Ser71, Asp72, Thr74, Tyr108, Ser174, Phe176, Pro188, Lys184, His200, Tyr294, Trp358) show the same side chain orientation as before (Figure 3A), with Lys184 again forming a covalent bond with the cofactor. Due to the higher resolution, Ser180 modeled slightly differently so that it now faces away from the phosphate moiety of the cofactor. The side chains of Arg75, Gln295, and Lys298 show minor variations among the three chains (Figure 3A). Several water molecules could now be placed with confidence, most importantly around the cofactor phosphate group.

The major novel findings derived from the new structure are observed adjacent to the nickel and the pyridinium ring. In the previously published structure for LarA, a large round density above the pyridinium ring was modeled as a sulfate molecule, potentially representing the lactate binding site.[2] In our new structure, we observe the same density; however, it occurs in three different variations in the three chains. In chain B the center of the density peak was ~3.4 Å away from the C4 of P2TMN and was again modeled as a sulfate molecule (Figure 3C), closely resembling the previous model. In chain A, however, the corresponding density was much closer to the ring, eliminating the possibility of modeling a sulfate which would lead to severe clashing in the structure. Considering that sulfite was used to protect LarA from oxidation and loss of nickel during purification and that sulfite can form a covalent adduct with C4 of NAD[26−28] and N5 of flavin,[29,30] we believe that the density represents a sulfite which is covalently linked to C4 of the pyridinium of the pincer cofactor. When sulfite donates its lone electron pair to C4, P2TMN converts into a reduced form. We therefore generated a model with sulfite

DOI: 10.1021/acs.biochem.8b00100
Biochemistry 2018, 57, 3244−3251

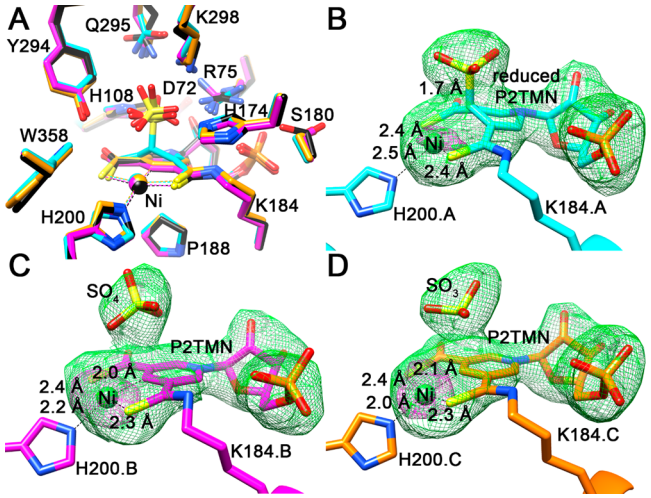

Figure 3. Comparison of the active sites of the LarA crystal structures. Carbon atoms are colored black for the closed conformation chain of the previous model (5HUQ); cyan for chain A, magenta for chain B, and light orange for chain C of the new structure (6C1W). (A) Active site based on C_α alignment of the four chains with active site residue side chains illustrated. Nickel atom and coordination colored as the corresponding carbon atoms. (B–D) Active sites of the three new chains with an $mF_o–F_c$ difference map shown for nickel, the cofactor and SO_3/SO_4 at 3σ in green. Anomalous map shown at 4σ in magenta. Nickel atoms are colored in light green. Nickel coordination is shown as black dashes with distances indicated. In B the C–S distance is labeled.

forming a covalent adduct with C4 of the reduced P2TMN, which nicely matched the $mF_o–F_c$ difference map of the omitted active site ligands after refinement (Figure 3B). The refined distance between the sulfur of sulfite and C4 of the cofactor (1.7 Å) is consistent with S–C bond formation. The position of the nickel atom also shifts slightly compared to the other chains. The resulting model indicates that the bond between nickel and the C4 atom is likely broken or largely weakened, and the interaction between nickel and His200 is also weaker, as this bond is now longer by ∼0.4 Å compared to other chains. It appears that nickel is less stable when P2TMN is in the reduced form. Indeed, when setting an occupancy of 1 for the nickel atom in chain A, the metal ion was refined to a B-factor ∼20 $Å^2$ higher than the surrounding atoms, a value that is also greater than what was measured for the other chains and consistent with the observed weaker anomalous signal. This result indicates that the nickel atom in chain A has a greater thermal mobility and/or that it has reduced occupancy. Finally, chain C was modeled as P2TMN and a sulfite molecule, with the C4–S distance too far to be a covalent bond, but too close for a sulfate that would sterically clash (Figure 3D). This active site appears to be an intermediate step before P2TMN reduction and formation of the C–S bond. Of potential relevance to the enzyme mechanism, the observation of a covalent adduct between sulfite and the nickel-pincer cofactor is a plausible mimic of the interaction between a hydride and the active site.

Computational Analysis of LarA. Computational studies suggested the hydride can transfer either to the C4 position of the pyridinium ring or to the nickel, but the latter occurs only if His200 dissociates. If the protonated or neutral form of His200

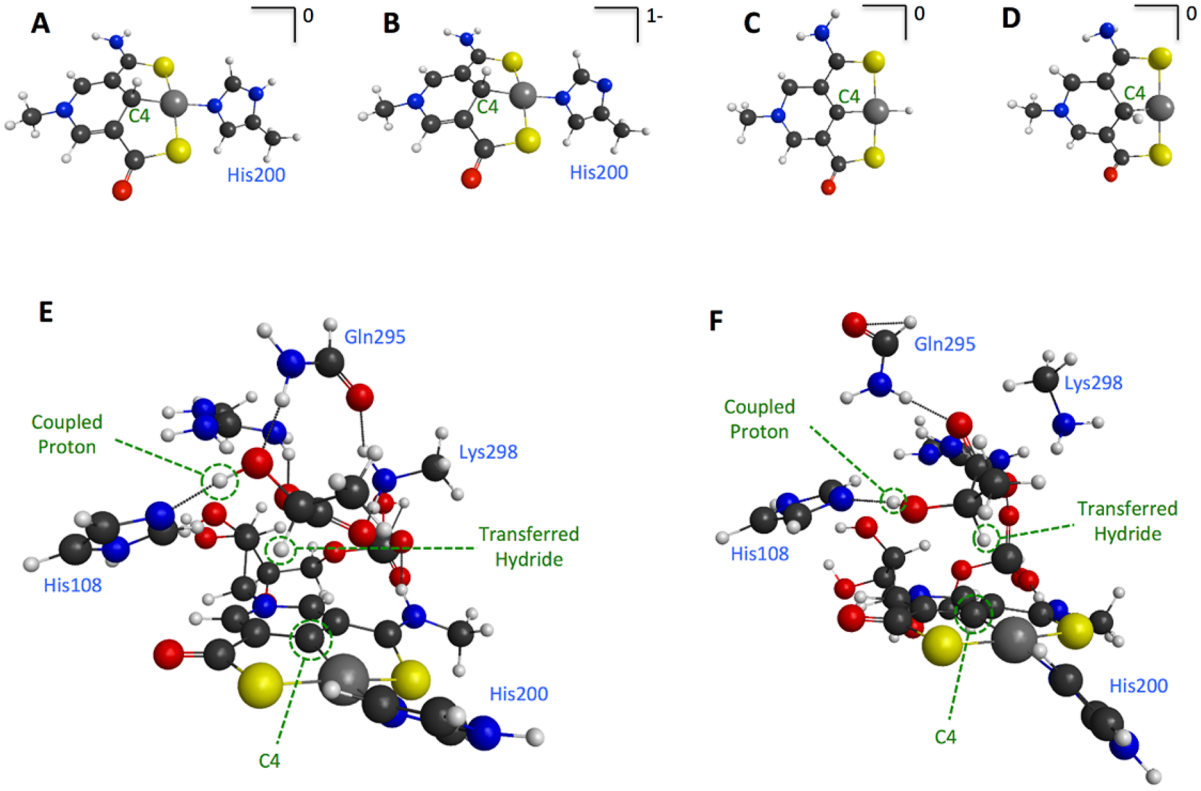

Figure 4. Models used to investigate hydride binding to the nickel-pincer cofactor. (A–D) Small models with hydride transfer to the C4 position and to the nickel. Large models (reactant geometries) obtained from the structures reported by (E) Zhang and Chung[11] or (F) Yu and Chen.[12] Colored as nickel, gray; sulfur, yellow; nitrogen, blue; oxygen, red; carbon, black; and hydrogen, white.

DOI: 10.1021/acs.biochem.8b00100
Biochemistry 2018, 57, 3244–3251

is coordinated to nickel, the hydride binds only to the C4 position (Figure 4A,B). For the model with dissociated His200, the hydride can bind to nickel (Figure 4C); however, the binding to the C4 atom (Figure 4D) is more favorable by 8.4 kcal/mol. We investigated the hydride transfer to C4 in more detail using the large models obtained from the structures reported by Zhang and Chung[11] (Figure 4E) and Yu and Chen[12] (Figure 4F). The transition states were calculated to be 24.5 and 14.6 kcal/mol above the reactants with models E and F, respectively (Table S2). These values are in good agreement with the 27.5 and 12.0 kcal/mol barriers reported for similar models and level of theory.[11,12] The significantly lower barrier predicted by model F is likely due to different orientations of Lys298 and Gln295, which stabilize the PCHT transition state.[12] The agreement between the predicted barrier for model F and the activation energy of 12.8 kcal/mol obtained from the experimental data,[14] as well as the lack of evidence for changing the nickel oxidation state provide strong support for the PCHT mechanism.

CONCLUSIONS

We have provided compelling evidence that LarA utilizes a PCHT rather than a PCET mechanism on the basis of (i) the lack of a Ni(III) EPR signal associated with the enzyme, (ii) the intermediacy of pyruvate upon quenching of the reaction, and (iii) the observation of a KIE when using 2-α-^{2}H-lactic acid thus demonstrating the breakage of this C−H bond. Consistent with a hydride transfer to the nickel-pincer cofactor, we observed a perturbation of the UV−visible spectrum upon addition of substrate to the enzyme. Additionally, sulfite addition caused changes to the UV−vis spectrum of LarA. A sulfite adduct at the C4 position of the cofactor was identified in a higher resolution crystal structure of LarA, compatible with hydride addition at this site. Finally, we used computational methods to calculate the energies of transition states and intermediates in the reaction. In contrast to similar prior calculations, we note that hydride transfer to Ni(II) is feasible if the His200 ligand dissociates during catalysis. Significantly, synthetic Ni-pincer complexes with hydride in the same plane as the pincer are well-known.[31−35] Our calculations using active site models and these synthetic compound precedents suggest that further investigation is needed to test for a nickel-hydride intermediate in LarA.

ASSOCIATED CONTENT

Supporting Information

The Supporting Information is available free of charge on the ACS Publications website at DOI: 10.1021/acs.biochem.8b00100.

Figure S1 providing liquid chromatography−mass spectrometry results for pyruvate detection and tables enumerating the crystal statistics of the LarA structure, absolute energies and atomic coordinates for large and small active site models (PDF)

AUTHOR INFORMATION

Corresponding Authors

*(J.M.) E-mail: mccracke@msu.edu.
*(J.H.) E-mail: hujian1@msu.edu.
*(S.A.V.) E-mail: svargonov@unr.edu.
*(R.P.H.) E-mail: hausinge@msu.edu.

ORCID

Joel A. Rankin: 0000-0002-9775-4508
Matthias Fellner: 0000-0003-3192-6984
Jian Hu: 0000-0001-6657-9826
Sergey A. Varganov: 0000-0001-8301-3891
Robert P. Hausinger: 0000-0002-3643-2054

Funding

This work was supported by the National Science Foundation (Grant CHE-1516126 to R.P.H. and J.H.; CAREER Award CHE-1654547 to S.A.V.)

Notes

The authors declare no competing financial interest.

ACKNOWLEDGMENTS

We thank Tony Schilmiller and Dan Jones of the Michigan State University Mass Spectrometry Core facility for advice on pyruvate detection.

REFERENCES

(1) Tatum, E. L., Peterson, W. H., and Fred, E. B. (1936) CCLXVI. Enzymic racemization of optically active lactic acid. *Biochem. J. 30*, 1892−1897.

(2) Desguin, B., Zhang, T., Soumillion, P., Hols, P., Hu, J., and Hausinger, R. P. (2015) A tethered niacin-derived pincer complex with a nickel-carbon bond in lactate racemase. *Science 349*, 66−69.

(3) Desguin, B., Soumillion, P., Hols, P., and Hausinger, R. P. (2016) Nickel-pincer cofactor biosynthesis involves LarB-catalyzed pyridinium carboxylation and LarE-dependent sacrificial sulfur insertion. *Proc. Natl. Acad. Sci. U. S. A. 113*, 5598−5603.

(4) Desguin, B., Goffin, P., Viaene, E., Kleerebezem, M., Martin-Diaconescu, V., Maroney, M. J., Declercq, J.-P., Soumillion, P., and Hols, P. (2014) Lactate racemase is a nickel-dependent enzyme activated by a widespread maturation system. *Nat. Commun. 5*, 3615.

(5) Fellner, M., Desguin, B., Hausinger, R. P., and Hu, J. (2017) Structural insights into the catalytic mechanism of a sacrificial sulfur insertase of the N-type ATP pyrophosphatase family, LarE. *Proc. Natl. Acad. Sci. U. S. A. 114*, 9074−9079.

(6) Desguin, B., Soumillion, P., Hausinger, R. P., and Hols, P. (2017) Unexpected complexity in the lactate racemization system of lactic acid bacteria. *FEMS Microbiol. Rev. 41*, S71−S83.

(7) Fellner, M., Rankin, J. A., Hu, J., and Hausinger, R. P. (2017) Lactate racemase, In *Encyclopedia of Inorganic and Bioinorganic Chemistry* (Scott, R. A., Ed.), p eibc2508, Wiley & Sons, West Sussex, U.K..

(8) Belenky, B., Bogan, K. L., and Brenner, C. (2007) NAD^+ metabolism in health and disease. *Trends Biochem. Sci. 32*, 12−19.

(9) Desguin, B., Soumillion, P., Hols, P., Hu, J., and Hausinger, R. P. (2017) Lactate racemase and its niacin-derived, covalently-tethered, nickel cofactor, In *The Biological Chemistry of Nickel* (Zamble, D. B., Rowinska-Zyrek, M., and Kozlowski, H., Eds.), pp 220−236, Royal Society of Chemistry, Cambridge, U.K..

(10) Xu, T., Wodrich, M. D., Scopelliti, R., Corminboeuf, C., and Hu, X. (2017) Nickel pincer model of the active site of lactate racemase involves ligand participation in hydride transfer. *Proc. Natl. Acad. Sci. U. S. A. 114*, 1242−1245.

(11) Zhang, X., and Chung, L. W. (2017) Alternative mechanistic strategy for enzyme catalysis in a Ni-dependent lactate racemase (LarA): Intermediate destabilization by the cofactor. *Chem. - Eur. J. 23*, 3623−3630.

(12) Yu, M.-J., and Chen, S.-L. (2017) From NAD^+ to Ni pincer complex: A significant cofactor evolution presented by lactate racemase. *Chem. - Eur. J. 23*, 7545−7557.

(13) Qiu, B., and Yang, X. (2017) Bio-inspired design and computational prediction of scorpion-like SCS nickel pincer complexes for lactate racemization. *Chem. Commun. 53*, 11410−11413.

DOI: 10.1021/acs.biochem.8b00100
Biochemistry 2018, 57, 3244−3251

(14) Wang, B., and Shaik, S. (2017) The nickel-pincer complex in lactate racemase is an electron relay and sink that acts through proton-coupled electron transfer. *Angew. Chem., Int. Ed. 56*, 10098−10102.
(15) Bradford, M. M. (1976) A rapid and sensitive method for the quantitation of microgram quantities of protein utilizing the principle of protein-dye binding. *Anal. Biochem. 72*, 248−254.
(16) Zhu, A., Romero, R., and Petty, H. R. (2010) A sensitive fluorimetric assay for pyruvate. *Anal. Biochem. 396*, 146−151.
(17) Wang, Z., Tang, S., Jin, Y., Zhang, Y., Hattori, M., Zhang, H., and Zhang, N. (2015) Two main metabolites of gentiopicroside detected in rat plasma by LC-TOF-MS following 2,4-dinitrophenylhydrazine derivatization. *J. Pharm. Biomed. Anal. 107*, 1−6.
(18) Otwinowski, Z., and Minor, W. (1997) Processing of X-ray diffraction data collected in oscillation mode. *Methods Enzymol. 276*, 307−326.
(19) Adams, P. D., Afonine, P. V., Bunkóczi, G., Chen, V. B., Davis, I. W., Echols, N., Headd, J. J., Hung, L.-W., Kapral, G. J., Grosse-Kunstleve, R. W., McCoy, A. J., Moriarty, N. W., Oeffner, R., Read, R. J., Richardson, D. C., Richardson, J. S., Terwilliger, T. C., and Zwart, P. H. (2010) *PHENIX*: A comprehensive Python-based system for macromolecular structure solution. *Acta Crystallogr., Sect. D: Biol. Crystallogr. 66*, 213−221.
(20) Emsley, P., Lohkamp, B., Scott, W. G., and Cowtan, K. (2010) Features and development of *Coot*. *Acta Crystallogr., Sect. D: Biol. Crystallogr. 66*, 486−501.
(21) Lebedev, A. A., Young, P., Isupov, M. N., Moroz, O. V., Vagin, A. A., and Murshudov, G. N. (2012) JLigand: A graphical tool for the CCP4 template-restraint library. *Acta Crystallogr., Sect. D: Biol. Crystallogr. 68*, 431−440.
(22) Pettersen, E. F., Goddard, T. D., Huang, C. C., Couch, G. S., Greenblatt, D. M., Meng, E. C., and Ferrin, T. E. (2004) UCSF Chimera–a visualization system for exploratory research analysis. *J. Comput. Chem. 25*, 1605−1612.
(23) Gordon, M. S., and Schmidt, M. W. (2005) Advances in Electronic Structure Theory: GAMESS a Decade Later, in *Theory and Applications of Computational Chemistry: The First Forty Years* (Dykstra, C. E., Frenking, G., Kim, K. S., and Scuseria, G. E., Eds.), pp 1167−1189, Elsevier, Amsterdam.
(24) Shapiro, S. S., and Dennis, D. (1965) Lactic acid racemization in *Clostridium butylicum*. Evidence for a direct hydride shift. *Biochemistry 4*, 2283−2288.
(25) Fersht, A. (1977) *Enzyme Structure and Mechanism*; W. H. Freeman and Company, New York.
(26) Johnson, S. L., and Smith, K. W. (1976) The interaction of borate and sulfite with pyridine nucleotides. *Biochemistry 15*, 553−559.
(27) Parker, D. M., Lodola, A., and Holbrook, J. J. (1978) Use of sulphite adduct of nicotinamide-adenine dinucleotide to study ionizations and the kinetics of lactate dehydrogenase and malate dehydrogenase. *Biochem. J. 173*, 959−967.
(28) Larsen, P. O., Sundahl, M., and Wieczorkowska, E. (1982) Hydride ion and sulfite ion attack on pyridine derivatives. *J. Chem. Educ. 59*, 1080−1081.
(29) Massey, V., Müller, F., Feldberg, R., Schuman, M., Sullivan, P. A., Howell, L. G., Mayhew, S. G., Matthews, R. G., and Foust, G. P. (1969) The reactivity of flavoproteins with sulfite. Possible relevance to the problem of oxygen reactivity. *J. Biol. Chem. 244*, 3999−4006.
(30) Tan, T.-C., Pitsawong, W., Wongnate, T., Spadiut, O., Haltrich, D., Chaiyen, P., and Divne, C. (2010) H-Bonding and positive charge at the N(5)/O(4) locus are critical for the covalent flavin attachment in *Trametes* pyranose 2-oxidase. *J. Mol. Biol. 402*, 578−594.
(31) Boro, B. J., Duesler, E. N., Goldberg, K. I., and Kemp, R. A. (2009) Synthesis, characterization, and reactivity of nickel hydride complexes containing 2,6-$C_6H_3(CH_2PR_2)_2$ (R = *t*Bu, *c*Hex, *i*Pr) pincer ligands. *Inorg. Chem. 48*, 5081−5087.
(32) Mock, M. T., Potter, R. G., O'Hagan, M. J., Camaioni, D. M., Dougherty, W. G., Kassel, W. S., and DuBois, D. L. (2011) Synthesis and hydride transfer reactions of cobalt and nickel hydride complexes to BX_3 compounds. *Inorg. Chem. 50*, 11914−11928.
(33) Rossin, A., Peruzzini, M., and Zanobini, F. (2011) Nickel(II) hydride and fluoride pincer complexes and their reactivity with Lewis acids BX_3·L (X = H, L = thf; X = F, L = Et_2O). *Dalton Trans. 40*, 4447−4452.
(34) Chierotti, M. R., Rossin, A., Gobetto, R., and Peruzzini, M. (2013) Interaction between a transition-metal fluoride and a transition-metal hydride: Water-mediated hydrofluoric acid evolution following fluoride solvation. *Inorg. Chem. 52*, 12616−12623.
(35) Wilson, G. L. O., Abraha, M., Krause, J. A., and Guan, H. (2015) Reactions of phenylacetylene with nickel POCOP-pincer hydride complexes resulting in different outcomes from their palladium analogues. *Dalton Trans. 44*, 12128−12136.

DOI: 10.1021/acs.biochem.8b00100
Biochemistry 2018, 57, 3244−3251